THE JOURNAL OF BIOLOGICAL CHEMISTRY
Vol. 279, No. 4, Issue of January 23, pp. 2913–2921, 2004
Printed in U.S.A.

Molecular Cloning and Functional Expression of zfCx52.6

A NOVEL CONNEXIN WITH HEMICHANNEL-FORMING PROPERTIES EXPRESSED IN HORIZONTAL CELLS OF THE ZEBRAFISH RETINA*

Received for publication, May 8, 2003, and in revised form, October 28, 2003
Published, JBC Papers in Press, October 28, 2003, DOI 10.1074/jbc.M304850200

Georg Zoidl‡, Roberto Bruzzone§, Svenja Weickert‡, Marian Kremer‡, Christiane Zoidl‡, Georgia Mitropoulou§, Miduturu Srinivas¶, David C. Spray¶, and Rolf Dermietzel‡‖

From the ‡Department of Neuroanatomy and Molecular Brain Research, Ruhr-University-Bochum, University Street 150, D-44801 Bochum, Germany, the §Department of Neuroscience, Institute Pasteur, 75015 Paris, France, the Department of Clinical Neurobiology, Interdisciplinary Center for Neurosciences (IZN), 69120 Heidelberg, Germany, and the ¶Department of Neuroscience, Albert Einstein College of Medicine, Rose F. Kennedy Center, Bronx, New York 10461

Gap junction-mediated electrical coupling contributes to synchronous oscillatory activities of neurons, and considerable progress has been made in defining the molecular composition of gap junction channels. In particular, cloning and functional expression of gap junction proteins (connexins (Cx)) from zebrafish retina have shown that this part of the brain possesses a high degree of connexin diversity that may account for differential functional properties of electrical synapses. Here, we report the cloning and functional characterization of a new connexin, designated zebrafish Cx52.6 (zfCx52.6). This connexin shows little similarity to known connexins from fish and higher vertebrates. By combining *in situ* hybridization with Laser Capture Microdissection and RT-PCR, we found that this novel fish connexin is expressed in horizontal cells in the inner nuclear layer of the retina. Functional expression of zfCx52.6 in neuroblastoma cells and *Xenopus* oocytes led to functional gap junctional channels and, in single oocytes, induced large non-junctional membrane currents indicative of the formation of hemichannels, which were inhibited in reversible fashion by raising extracellular Ca^{2+} concentrations.

A wealth of knowledge concerning the molecular composition and functional properties of non-neuronal gap junctions has been accumulated (for review, see Refs. 1–3). In contrast, the identity and role of connexins present at neuronal gap junctions have been less well defined (4–6). Electrical synapses (gap junctions) in neuronal circuits have become a major focus in the study of network properties such as synchronization and oscillation (7, 8). Knowledge of the full connexin complement expressed by neurons of the central nervous system is an essential prerequisite to our understanding of the contribution of electrical synapses to these fundamental properties of network functioning. The first neuronal connexin was identified by O'Brien *et al.* (9), who used a skate retina expression library to clone fish connexin35 (Cx35),[1] a protein of 35-kDa molecular mass, preferentially expressed in the inner nuclear (INL) and inner plexiform layers (IPL) of fish retina (10). Transcripts of the murine ortholog, Cx36, have been detected in the inferior olive, reticular thalamus, multiple retinal neurons, inhibitory interneurons of the neocortex, and the hippocampal formation (11–17). More recently, we have demonstrated the differential expression of other connexin genes in the fish retina, namely zebrafish Cx55.5 (zfCx55.5), zfCx44.1, zfCx27.5, and carp Cx43 (18).

The retina is a highly ordered laminar structure, comprising three compact layers of neurons separated by two synaptic layers, which has proven a valuable model to study gap junctions and cell specific expression patterns of connexins in neuronal tissues (19, 20). Gap junction-mediated dye transfer is found between nearly all cell types that form the neuronal retinal matrix (21–24) and a diversity of coupling patterns that is so far unmatched in any other part of the brain (25, 26). More recently, direct demonstration of electrical and metabolic communication between different classes of retinal neurons has been obtained (16, 27–30). The selective nature of neuronal coupling and its differential regulation by neuromodulators (31–37), as shown recently for the amacrine AII cells (23, 38, 39), supports the idea that multiple types of connexins may exist within the neuronal populations of this tissue.

We have recently described a molecular approach to clone novel connexin genes from primary neurons of fish retina, taking advantage of a dissociation procedure that allows for >70% enrichment of horizontal cells (18). By combining rapid amplification of cDNA ends (RACE) with the screening of a genomic DNA library from zebrafish, we have isolated a novel connexin gene, designated as zfCx52.6 because of its predicted molecular mass. Sequence analysis revealed only limited homology to other connexins from fish and higher vertebrates, indicating that zfCx52.6 is a distant relative of the known connexin genes. *In situ* hybridization, laser capture microdissection (LCM) and RT-PCR analysis demonstrated that this connexin is specifically expressed in the INL of the retina. During development the up-regulation of zfCx52.6 expression parallels the expression profile of the basic helix loop helix transcription factor atonal5, an established marker for retinogenesis (40). Functional expression studies in transiently

* This work was supported by the Deutsche Forschungsgemeinschaft, SFB 509, National Institutes of Health Grant MH65495, and the Association RETINA France. The costs of publication of this article were defrayed in part by the payment of page charges. This article must therefore be hereby marked "*advertisement*" in accordance with 18 U.S.C. Section 1734 solely to indicate this fact.

The nucleotide sequence(s) reported in this paper has been submitted to the GenBank™/EBI Data Bank with accession number(s) GI:21311548.

‖ To whom correspondence should be addressed. Tel. 49-234-322-5003; Fax: 49-234-321-4655; E-mail: rolf.dermietzel@ruhr-uni-bochum.de.

[1] The abbreviations used are: Cx35, connexin35; RACE, rapid amplification of cDNA ends; TM, transmembrane; INL, inner nuclear layer; IPL, inner plexiform layer; ONL, outer nuclear layer; OPL, outer plexiform layer; GCL, ganglion cell layer; LCM, laser capture microdissection.

transfected Neuro2A as well as single or paired *Xenopus* oocytes indicated that it is a functional member of the connexin family that exhibited a moderate degree of voltage sensitivity, a unitary conductance of 41 ± 3 pS and the formation of Ca^{2+}-gated hemichannels. Expression, localization and biophysical properties suggest that zfCx52.6 is a candidate zebrafish horizontal cell gap junction protein.

MATERIALS AND METHODS

Cloning of Full-length zfCx52.6—A full-length clone of zfCx52.6 was obtained by screening a zebrafish genomic library (Stratagene, La Jolla, CA) with the probe frag50 previously described (18). The genomic clone was sequenced, and RACE extension, using retina RNA as the template, was performed to identify expressed sequences from the zfCx52.6 genomic locus. The molecular procedures used have been described in detail previously (18, 41, 42). The zfCx52.6 gene sequence was deposited in GenBank™ (GI:21311548).

The zfCx52.6 DNA, mRNA, and protein structures were analyzed with the Lasergene software (DNASTAR, Madison, WI), the protein prediction and analysis tools at the ExPasy home page (www.expasy.ch), SMART (smart.embl-heidelberg.de), and Predictprotein (www.embl-heidelberg.de/-predictprotein/). Putative phosphorylation motifs were predicted using Phosphobase 2.0 (www.cbs.dtu.dk).

RNA Isolation and RT-PCR Analysis—Total RNA was isolated from adult zebrafish tissues and developmental stages after lysis in TRIzol reagent according to the manufacturer's protocol (Invitrogen Corp., Carlsbad, CA) and first-strand cDNA synthesized as described by Zoidl *et al.* (43). ZfCx52.6 expression was detected by RT-PCR using upstream (sense) primer Cx52.6-1 (5′-CTCGGCCGACAGAGAAGAACATC-3′) and downstream (antisense) primer Cx52.6–2 (5′-TCACTGCTGCAGGATTGCAGACG-3′). The primers for β-actin (actin-1, nt 226–246, actin-2, nt 448–429) have been described previously (18). The cDNA equivalent of 1 ng of total RNA was used as the template for a PCR reaction (50 μl of total volume) in a mixture containing: 20 mM Tris-HCl, pH 8.4, 50 mM KCl, 1.5 mM $MgCl_2$, 0.2 mM dNTPs, 25 pmol of specific primers, and 2.5 units of TaqDNA-polymerase (Applied Biosystems, Foster City, CA). To ensure that PCR signals were not the result of contaminating genomic DNA, control samples containing either water or RNA, in which the reverse transcriptase was omitted from the step of cDNA synthesis, were run in parallel. An initial denaturation step at 94 °C for 2 min was followed by 35 amplification cycles (30 s at 94 °C; 30 s at 52 °C; 30 s at 72 °C) and a final extension period of 10 min at 72 °C. Volumes of 10 μl of each amplification reaction were separated on 1% agarose gels and images of ethidium bromide-stained gels were recorded using the Imagemaster documentation system (AP-Biotech, Piscataway, NJ).

Real time RT-PCR was performed using the 2× Real-time SYBR-Green I Kit (Eurogentec SA, Seraing, Belgium) and the reaction conditions described recently (44). Primers were selected using the Primer Express®Software (Applied Biosystems). The sense and antisense primers for actin were actin-3 (5′-ACTCCATCATGAAGTGCG-ACG-3′) and actin-4 (5′-TTCCTTCTGCATACGGTCAGC-3′). The sense and antisense primers for zfCx52.6 were zfCx52.6–3 (5′-TGGACAGATGG-TACCTTTGCC-3′) and zfCx52.6–4 (5′-GTTGTCTGG-AATGGACCT-TCG-3′). The primers for atonal5 (ath5; GI:10566824), notch homolog 1a (notch1a; GI:10859115) and 16 S ribosomal RNA (16s rRNA; GI: 4835956) were Ath5–1 (5′-CGGCCAATGCAAGAGAACGAAAGA-3′) and Ath5–2 (5′-TCCGATTGAGGGCCATGAT-GTAGCT-3′), notch1a-1 (5′-CCCCGCTC-TGCTGCCCAAACA-3′), notch1a-2 (5′-TTGCG-TGT-TTTCTTAGCCGTGTTGTTGT-3′), 16s-1 (5′-GGGGCGACCACGGAG-TAAAAAACA-3′) and 16s-2 (5′-GGCCGGATCGTCTTTGGTCAGGT-3′). The threshold cycle (Ct-value) was determined as the first amplification cycle with a signal above background. The relative level of zfCx52.6 expression was calculated using the ΔCt-Method using actin or 16 S rRNA expression as the endogenous reference (Applied Biosystems). The different expression levels were graphically expressed as the ΔCt value that was calculated by subtraction of the mean Ct value of the reference gene (actin, 16s rRNA) from the mean Ct value of the gene of interest (zfCx52.6, notch1, zath5). All experiments shown represent two independent sets of samples. Each sample was analyzed in triplicate. Intraassay and interassay variability was less then 5%.

In Situ Hybridization and Laser Capture Microdissection Analysis—For the localization of zfCx52.6 in the zebrafish retina, *in situ* hybridization and RT-PCR analysis of laser microdissected samples were performed. Freshly prepared zebrafish eyes were embedded in Tissue-Tek (Miles, Elkhart, IN), frozen, and stored at −80 °C. Serial cryostat sections of 12-μm thickness were collected on superfrost plus slides (Menzel-Gläser, Braunschweig, Germany) and stored immediately at −80 °C. The *in situ* hybridization was performed essentially as described previously except for the anti-DIG antibody incubation step that was performed for 16 h at 4 °C (45). The antisense probe and the corresponding sense probe were generated from a plasmid containing nt 648–1401 of the zfCx52.6 coding region. The synthesized probe was selected for minimal homologies with published connexin sequences (GenBank™, NCBI, Washington, D. C.). All cRNA probes were hybridized to sections in 50 μl of hybridization buffer for 16 h. Probe concentrations (800 ng/ml) and temperature of pre-hybridization and hybridization (52 °C) were selected for high stringency. After digestion of excess RNA and color development samples were counterstained with Certistain ("Kernechtrot"; VWR International AG, Switzerland) for 1min and mounted in aqueous mounting medium (Shandon, Frankfurt, Germany).

For laser capture microdissection, 7-μm cryostat sections were mounted on glass slides covered with polyethylene film (P.A.L.M., Bernried, Germany) and stored at −80 °C until use. After thawing, tissue sections were fixed in 100% ethanol for 2 min, air-dried, stained with toluidine blue (0.5%) for 10 s and dehydrated with sequential immersion in 70% ethanol and 100% ethanol, for 1 min each. After air-drying, the ganglion cell layer (GCL), IPL, INL, and outer nuclear/plexiform layer (ONL/OPL) were laser-microdissected using the UV-Cut system (SL-Microtest, Jena, Germany). RNA isolation was performed using the PureScript Kit (Gentra, Minneapolis, MN) with slight modifications to the manufacturer's recommendations for the 0.2–5 mg animal tissue protocol (www.gentra.com). Samples were picked with sterile injection needles (27-gauge × 3/4′, Braun-Melsungen, Melsungen, Germany) after laser microdissection and transferred into 0.5-ml reaction tubes containing 100 μl of cell lysis solution of the PureScript Kit and 1 μl of proteinase K (20 mg/ml) and incubated for 20 min at 42 °C. Following the addition of DNA precipitation solution (33 μl), samples were incubated on ice for 5 min and then centrifuged for 20 min at room temperature. The supernatant was collected and 100 μl of isopropyl alcohol plus 1 μl of glycogen (10 mg/ml) was added. After incubation at −20 °C for 30 min, samples were centrifuged at 4 °C for 30 min. The pellet was washed with 100 μl of 70% ethanol, air-dried, and resuspended in 15 μl of DEPC-treated water. RT-PCR was performed using the Qiagen OneStep RT-PCR Kit (Qiagen, Hilden, Germany). Reactions were set up in a 20-μl volume, using Q-solution according to the manufacturer's protocol. For detection of zfCx52.6, the zfCx52.6–1 and zfCx52.6–2 primers described above (see RNA isolation and RT-PCR analysis) were used, whereas those for the control reaction were the actin-1 and actin-2 primers. The reverse transcription reaction was carried out for 30 min at 50 °C. Then followed a denaturation step of 15 min at 95 °C, and 50 cycles of 94 °C for 30 s, 55 °C for 30 s, 72 °C for 1 min. Aliquots (15 μl) from each amplification reaction were separated on 2.5% agarose gels and images of ethidium bromide-stained gels were recorded using Imagemaster (AP-Biotech).

Electrical Recordings from Neuro2A Cells—The full-length zfCx52.6 cDNA (nt 1–1401) including the stop codon was cloned into the plasmid pCR3.1 (Invitrogen) by TA-cloning. The Neuro2A cell line (46) was cultured and transiently transfected as described in detail previously (47). Transfected cells were dissociated at 8–12 h after transfection and plated at low density on 1-cm round glass coverslips. Junctional conductance was measured between cell pairs by using the dual whole cell voltage clamp technique with Axopatch 1D patch-clamp amplifiers (Axon Instruments, Foster City, CA) at room temperature. The solution bathing the cells contained 140 mM NaCl, 5 mM KCl, 2 mM CsCl, 2 mM $CaCl_2$, 1 mM $MgCl_2$, 5 mM Hepes, 5 mM dextrose, 2 mM pyruvate, and 1 mM $BaCl_2$, pH 7.4. Patch electrodes had resistances of 3–5 MΩ when filled with internal solution containing 130 mM CsCl, 10 mM EGTA, 0.5 mM $CaCl_2$, 3 mM MgATP, 2 mM Na_2ATP, and 10 mM Hepes, pH 7.2. Single-channel recordings were filtered at 0.2–0.5 kHz and sampled at 1–2 kHz. Data were acquired by PCLAMP8 software (Axon Instruments); analysis was performed with PCLAMP8 and ORIGIN 6.0 software (Microcal Software, Northampton, MA). Each cell of a pair was initially held at a common holding potential of 0 mV. Single-channel currents were investigated in weakly coupled cell pairs (1 or 2 channels) without the use of uncoupling agents by applying 8–16 s voltage pulses between +100 and −100 mV to one cell of a pair to establish a transjunctional voltage gradient (V_j) while the junctional current was measured in the second cell (held at 0 mV). Gating events were recognized as simultaneously occurring events of equal amplitude and opposite polarity in current traces for both cells in the pair. All point amplitude histograms of data were constructed at each voltage and fit to Gaussian functions to determine the mean and variance of the baseline and open channel current. Unitary conductances were measured by fitting a

linear function to the single-channel current-voltage relation.

In Vitro Transcription and Translation of zfCx52.6—The entire coding sequence of zfCx52.6 was amplified by polymerase chain reaction (PCR) with primers corresponding to nucleotides 1–19 (sense: 5′-GGGT-CCAGGAATTCATGGGAGATTGGAACTTGC-3′) and 1401–1382 (antisense: 5′-GC-CCCGGCTCGAGTCAGAATTTTCTTACCATT-3′), containing EcoRI (sense) and XhoI (antisense) linkers. PCR products were purified using Qiaquick columns (Qiagen), digested with EcoRI/XhoI (Roche Applied Science), purified by agarose gel electrophoresis and subcloned into the corresponding sites of the pCS2+ expression vector. The construct was sequenced using the Dye terminator (Applied Bioystems), as recommended by the manufacturer, to verify that PCR amplification did not introduce unwanted mutations.

Recombinant plasmid was linearized with NotI (Roche Applied Science), gel purified, and used as template (1–2 μg of DNA) to produce capped RNA using the mMessage mMachine kit (Ambion, Austin, TX). The purity and yield of transcribed cRNA was determined by measuring absorbance at 260/280 nm. Aliquots (200 ng) of *in vitro* synthesized connexin RNA were translated (1 h at 30 °C) in a rabbit reticulocyte lysate (Promega, Madison, WI) in the presence of [^{35}S]methionine (ICN Pharmaceuticals, Costa Mesa, CA; 30 μCi/tube) and reactions were quenched by dilution in gel sample buffer (25 mM Tris-HCl, pH 6.8, 0.5% SDS, 0.1% β-mercaptoethanol, 17% glycerol, 0.01% bromphenol blue). Radioactive products (1/10 of the reaction volume) were separated by electrophoresis on a 13% SDS-polyacrylamide gel, fixed in 10% acetic acid/20% methanol for 30 min, soaked in 1 M sodium salicylate for 30 min at room temperature, dried, and visualized by fluorography (Hyperfilm, AP-Biotech).

Preparation, Microinjection, and Pairing of Oocytes—Female *Xenopus laevis* were purchased from the colony of the Institut für Entwicklungsbiologie (Hamburg, Germany). Following anesthesia with benzocaine, ovarian lobes were surgically removed and placed in Modified Barth's medium (MB: 110 mM NaCl, 1.3 mM KCl, 3 mM $NaHCO_3$, 19 mM HEPES, 0.9 mM $MgSO_4$, 0.4 mM $CaNO_3$, 0.5 mM $CaCl_2$, pH 7.6) at 18 °C overnight. Oocytes were isolated and defolliculated by enzymatic digestion and cultured in Modified Barth's medium at 18 °C, essentially as previously described (48, 49). For physiological analysis, cells were injected with a total volume of 40 μl of either an antisense oligonucleotide (2.5 ng/cell) to suppress the endogenous *Xenopus* Cx38 (XenCx38), or a mixture of antisense (as above) plus zfCx52.6 RNA (10–40 ng/cell), using a Picospritzer II (General Valve Corporation, Fairfield, NJ). Following an overnight incubation at 18 °C, microinjected oocytes were immersed for a few minutes in hypertonic solution to strip the vitelline envelope (50), transferred to Petri dishes containing MB medium and manually paired with the vegetal poles apposed.

Electrical Recordings from Oocytes—All experiments were carried out at 18 °C. The functional properties of cell-to-cell channels were assessed by a dual voltage clamp procedure that enables direct quantification of junctional conductance (51). Current and voltage electrodes (1.2 mm in diameter, Omega dot; Glass Company of America, Millville, NJ) were pulled to a resistance of 1–2 MΩ with a horizontal puller (PB-7, Narishige, Tokyo, Japan) and filled with a solution containing: 3 M KCl, 10 mM EGTA, and 10 mM HEPES, pH 7.4. Voltage clamping of oocyte pairs was performed using two GeneClamp 500 amplifiers (Axon Instruments, Foster City, CA) controlled by a PC-compatible computer through a Digidata 1200 interface (Axon Instruments). pCLAMP 8.0 software (Axon Instruments) was used to program stimulus and data collection paradigms. Current outputs were filtered at 50 Hz and the sampling interval was 10 ms. For simple measurements of junctional conductance, both cells of a pair were initially clamped at −40 mV to ensure zero transjunctional potential and alternating pulses of ± 10–20 mV were imposed to one cell. Current delivered to the cell clamped at −40 mV during the voltage pulse was equal in magnitude to the junctional current, and was divided by the voltage to yield the conductance.

To determine the voltage-gating properties of zfCx52.6, transjunctional potentials (V_j) of opposite polarity were generated by hyperpolarizing or depolarizing one cell in 20 mV steps (over a range of ±100 mV), while clamping the second cell at −40 mV. Currents were measured 10 s after the onset of the voltage pulse. At that time they approached steady state (I_{jss}), and the macroscopic conductance (G_{jss}) was calculated by dividing I_{jss} by V_j. G_{jss} was then normalized to the values determined at ±20 mV, and plotted against V_j. Data describing the relationship of G_{jss} as a function of V_j were analyzed using Microcal Origin 6.0 (Microcal Software, Northampton, NA) and fit to a Boltzmann relation of the form: $G_{jss} = \{(G_{jmax} - G_{jmin})/(1 + \exp[A(V_j - V_0)]\} + G_{jmin}$, where G_{jss} is the steady-state junctional conductance, G_{jmax} (normalized to unity) is the maximum conductance, G_{jmin} is the residual conductance at large values of V_j, and V_0 is the transjunctional voltage at which $G_{jss} = (G_{jmax} - G_{jmin})/2$. The constant A (= nq/kT) represents the voltage sensitivity in terms of gating charge as the equivalent number (n) of electron charges (q) moving through the membrane, k is the Boltzmann constant, and T is the absolute temperature. The junctional conductance of oocyte pairs selected for analysis of voltage sensitivity never exceeded 6 μS, thereby ensuring adequate control of transjunctional potential and avoiding the risk of overestimating the actual G_j at steady state (52). To characterize the hemichannel activity of non-junctional connexons, recordings were obtained from single oocytes with a two-electrode voltage-clamp procedure. Cells were clamped at −40 mV, and whole cell currents were recorded in response to depolarizing voltage steps (−20 to +60 mV at 20-mV intervals) imposed for a duration of 10 s. Current values recorded for 0.1 s at the end of the pulse were averaged and the increase above holding currents (ΔI_m) was plotted against the membrane potential. Oocytes were placed on Teflon tubing in a perfusion chamber and media were exchanged using an electronically controlled gravity flow perfusion system (ALA Scientific Instruments, Westbury, NY). All data were analyzed using Clampfit 8.0 (Axon Instruments) and data fitting functions in Origin 6.0 (Microcal Software) software.

Statistical Analysis—Results are shown as the mean ± S.E. Comparisons between two populations of data were made with the paired and unpaired Student's t tests where appropriate; p values of 0.05 or less were considered to be significant.

RESULTS

Cloning of zfCx52.6—An open reading frame of 1398 nt encoding a protein of 466 amino acids was identified by screening a zebrafish genomic library with the probe frag50. The probe has led to the discovery of zfCx55.5 as described previously by Dermietzel *et al.* (18). The new protein, with a deduced molecular weight of 52,611.5, was designated as zfCx52.6. Analysis of the zfCx52.6 sequence revealed the typical structure of a connexin protein with four transmembrane domains (TM) at positions 20–41 (TM1), 77–97 (TM2), 164–182 (TM3), and 209–227 (TM4). ZfCx52.6 has a calculated pI of 8.77 and exhibits an unusual high content of the amino acid serine in the C-terminal domain of the protein, amounting to >11% of all amino acids. The majority of putative phosphorylation sites for the protein kinases calmodulin kinase II (CaMKII), casein kinase (CKII), protein kinase A (PKA), protein kinase C (PKC), protein kinase G (PKG), and glycogen synthase kinase 3 (GSK3) were predicted to occur in the C-terminal tail, suggesting that post-translational modifications may occur in particular in this domain.

A remarkable conservation of amino acids in the transmembrane domains was identified by alignments of the amino acid sequences of the novel zebrafish connexin with other mammalian connexins. This included a highly conserved proline at amino acid position 88 lining the second transmembrane domain and the charged or polar residues within the third transmembrane region, that have been postulated to represent the putative amphipathic strand that is thought to participate in the lining of the junctional channel, (53, 54). Furthermore, cysteine residues within the extracellular loops EL1 and EL2 are highly conserved.

The phylogenetic relationship of Cx52.6 to known zebrafish connexin genes revealed only limited homologies to the recently described zfCx55.5 (57% amino acid identity; GI:18858503) and zfC48.5 (51% amino acid identity; GI:21702716). Homologies to other zebrafish connexins were below 50% identity, indicating a clear evolutionary distance of zfCx52.6 to other known zebrafish connexin genes. No evolutionary relationship was observed to connexin genes cloned from other fish species (data not shown).

A BLASTP 2.2.6 analysis (55) using default parameters showed that zfCx52.6 is a novel member of the α-class of gap junction proteins. Upon alignment of the protein sequences, zfCx52.6 showed the best identity scores at the amino acid level to human Cx62 (GI:14009611; 48%), mouse Cx57 (GI:

FIG. 1. **Evolutionary relationship of zfCx52.6.** Amino acid alignment of zfCx52.6 (GI,21311549), human Cx62 (GI,15990855), human Cx59 (GI,13124059), and mouse Cx57 (GI,4582689) using the ClustalW analysis tool. *Stars* indicate amino acid identities, (+) indicates a conserved amino acid exchange, and (.) indicates no identity. The conserved amino acids proline and cysteine are shown in *bold letters*.

13124105; 47%) and human Cx59 (GI:13124059; 61%) (Fig. 1). Similarities between the novel connexin and other family members reside within the first 250 amino acids, whereas the C-terminal tail showed no significant homology to any known connexin of higher vertebrates.

Expression of zfCx52.6 in the Adult and Developing Zebrafish—The expression of zfCx52.6 was initially studied by RT-PCR analysis on samples of total RNA isolated from adult zebrafish brain, heart, kidney, lens, liver, and spleen (Fig. 2*A*). As shown, the zfCx52.6 transcript was detectable only in zebrafish retina, indicating the absence or very low mRNA abundance of this connexin in the other tissues tested. The steady state levels of the actin transcript were similar in all samples examined, demonstrating that equivalent amounts of cDNA were used in the PCR reactions.

Comparison of the amounts of zfCx52.6 mRNA in retina relative to potentially basal expression levels in other tissues was determined using the sensitive Quantitative Real-Time RT-PCR technique. A threshold value (Ct-value) for zfCx52.6 in retina of 29.45 + 0.4 cycles was measured in triplicate samples from two independent experiments. In contrast, the Ct-values for the other tissues examined were substantially higher (mean Ct-value: 35.82 + 1.3), indicating lower expression levels. Control experiments did not reveal any significant differences in steady state actin mRNA levels. The mean Ct-values for actin in the retina and all other tissues were 27.1 + 0.3 and 26.7 + 1.7, demonstrating that similar amounts of cDNA were included in the PCR reactions. The difference in relative expression values is summarized in Fig. 2*B*. This result confirmed the initial observation by qualitative RT-PCR that zfCx52.6 is

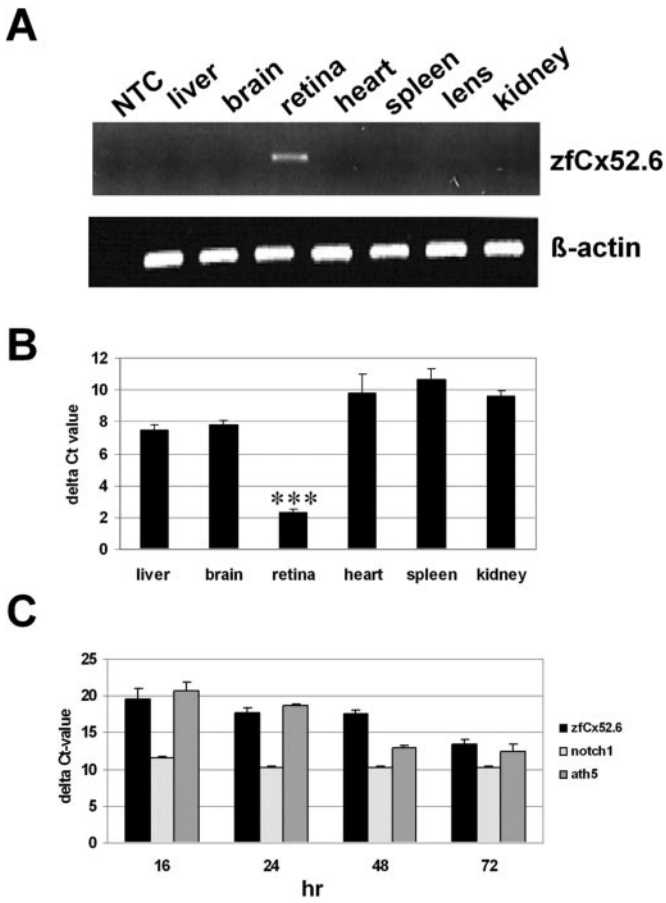

FIG. 2. **Tissue-specific expression and developmental regulation of zfCx52.6.** *A*, RT-PCR analysis of zfCx52.6 mRNA showed expression in the retina, whereas none of the other organs revealed detectable levels. The amplification product generated (453 bp) represents nt 605–1058 of the zfCx52.6 open reading frame. All cDNA preparations were assessed by PCR using primers specific for β-actin. This analysis confirmed that comparative amounts of cDNA were included in all the PCR reactions. *NTC* refers to the no template control. A second PCR control reaction (with β-actin primers) omitting reverse transcription produced no amplification products, indicating the absence of genomic DNA contamination in the mRNA samples (data not shown). *B*, graphical representation of the quantification of zfCx52.6 expression in adult zebrafish tissues by real time RT-PCR analysis. *C*, graphical representation of zfCx52.6 expression in the developing zebrafish embryo. Steady state mRNA levels were determined at selected time points and the expression of zfCx52.6 compared with the expression of the differentiation markers atonal5 (ath5) and notch1. The 16 S rRNA levels served as endogenous reference. The values given in *B* and *C* are calculated using the ΔCt method. Note that small values represent more abundant expression (***, $p < 0.001$), *error bars* indicate S.D.

highly expressed in the retina and showed that this connexin is at least 32-fold more abundant in retina as compared with other tissues.

The onset of zfCx52.6 expression was determined in zebrafish embryos collected at 1-h time intervals from 4 to 11 h and after 16, 24, 48 and 72 h. Embryos were staged according to Kimmel *et al.* (56), and total RNA isolated from homogenous whole embryo samples. ZfCx52.6 mRNA was detectable at low levels from 4 to 48 h (mean Ct values <32) but rose substantially after 48 h (mean Ct-value at 48 h: 32.34 ± 0.75). At 72 h (mean Ct-value: 27.77 ± 0.31) zfCx52.6 was increased slightly less than 32-fold when compared with the 48-h time point (Fig. 2*C*). Up-regulation of zfCx52.6 mRNA followed up-regulation of the expression of the zebrafish atonal5 gene (zath5) with a 24-h delay. Zath5, which is a known marker for neuronal differentiation in the retina (40), showed a more than 100-fold increase between 24 to 72 h. In contrast, notch1a gene expression, a

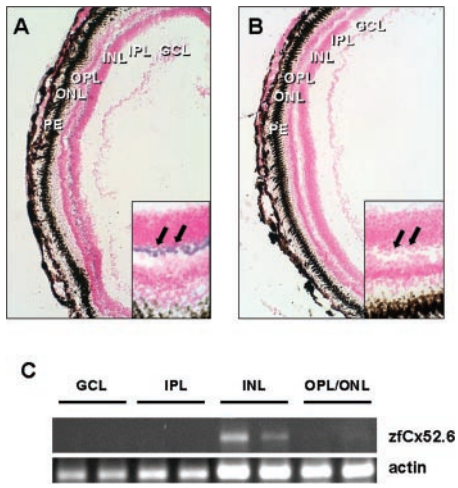

FIG. 3. **Localization of zfCx52.6 in the zebrafish retina.** *In situ* hybridization experiment using the antisense (*A*) and sense probe (*B*) derived from plasmid zfCx52.6 (nt 648–1401). zfCx52.6 reactive signals were visible at the border between INL and OPL. Note, that no signal was detectable with the sense control probe using the conditions outlined. *C*, RT-PCR analysis of cell groups derived from LCM. Two independent samples derived from each cell layer were subjected to RT-PCR. Actin reactions served as control for successful RNA extraction and to monitor the amount of cDNA included in individual RT-PCR reactions. *PE*, pigment epithelium. Sections were counterstained with Certistain ("Kernechtrot") to visualize cell nuclei.

marker for gliogenesis in the retina (57) did not show any significant change. This suggested that zfCx52.6 expression is linked to neurogenesis and/or retinogenesis in the zebrafish embryo.

Retinal Localization of zfCx52.6—An interesting question arising from the molecular cloning of multiple connexins from the fish retina is whether zfCx52.6 shows a cell specific pattern indicative of expression in distinct types of retinal neurons. To resolve positive signals at the single cell level, *in situ* hybridization studies using digoxigenin-labeled cRNA probes were performed. When cRNA probes specific for zfCx52.6 were used (Fig. 3*A*), labeling occurred at the border between inner nuclear layer (INL) and outer plexiform layer (OPL). The labeling pattern of zfCx52.6 revealed a restriction to linearly arrayed cell bodies at the border between the inner nuclear layer and the outer plexiform layer at sites where horizontal cells are expected to be localized. No signal was observed with the control sense riboprobes (Fig. 3*B*).

Since *in situ* hybridization experiments for detection of connexin genes have proven highly prone to cross-hybridization artifacts that cannot be fully overcome by extensive RNase digestion, increase in hybridization temperature or probe concentrations,[2] we used an independent detection method to verify the results of the *in situ* hybridizations. LCM was applied to collect cells from individual retina cell layers except for the OPL, which was not clearly separable by this method from the ONL. The samples were subjected to RNA extraction and used for RT-PCR analysis. As shown in Fig. 3*C*, zfCx52.6 expression was detectable only in the INL layer. No amplicon was obtained for the GCL, IPL, and OPL/ONL layers, excluding cross-hybridization with other mRNAs.

Functional Expression of zfCx52.6 in Neuro2A Cells—The neuroblastoma cell line Neuro2A (46) was selected for single channel studies by transient transfection with zfCx52.6. In this construct, amino acids 1–466 of zfCx52.6 were expressed under the control of the cytomegalovirus promoter. In order to permit visualization of transfected cell pairs co-transfections with an

[2] R. Dermietzel, unpublished observations.

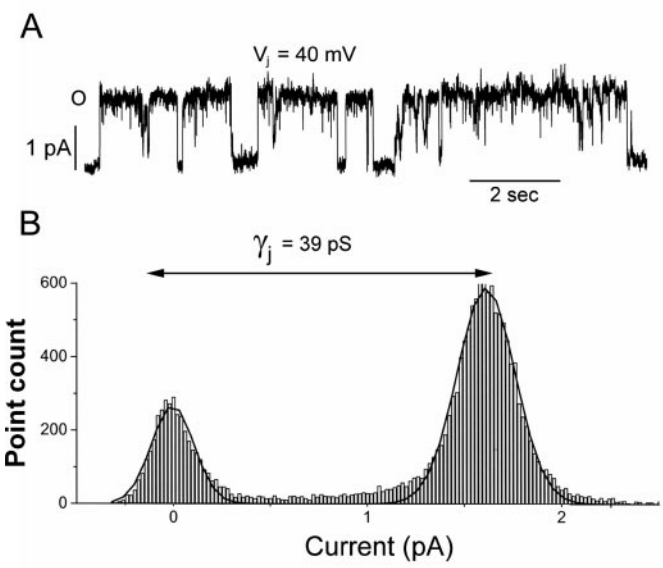

FIG. 4. **Single channel currents recorded from a pair of zfCx52.6 transfected Neuro2A cells.** *A*, current transitions from fully open (0) to closed states in a cell pair exhibiting a single active channel in response to transjunctional voltage (Vj) = 40 mV. *B*, all points histogram of trace in *A*, where peaks indicate currents corresponding to open and closed channels; the unitary conductance (γ_j, calculated as the difference in current between these peaks divided by transjunctional voltage) is 39 pS.

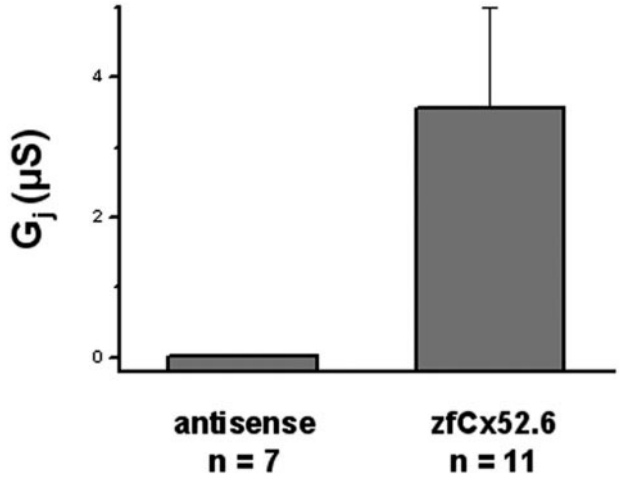

FIG. 5. **Expression of zfCx52.6 induces the formation of homomeric intercellular channels.** Oocytes pretreated with an oligonucleotide antisense to a sequence within the coding region of XenCx38 were injected with either zfCx52.6 RNA or water (antisense) and paired for 24–48 h before measuring junctional conductance by dual voltage clamp. Values are the mean ± S.E. of the indicated number of pairs from at least three separate batches of oocytes.

EGFP expression vector were performed as described in the methods. A representative recording from a cell pair at a Vj of 40 mV is illustrated in Fig. 4*A* and the corresponding all points histogram is illustrated in Fig. 4*B*. At this voltage the channels were open for 60 to 70% of the time. The all points histogram exhibited peaks at 0 pA and 1.56 pA, corresponding to the closed and open states, respectively, indicating a single channel conductance of 39 pS. Single channel current-voltage (I-V) relations from three different cell pairs with single active channels in response to voltage pulses indicated that the unitary conductance of zfCx52.6 channels was 41 ± 3 pS.

Functional Expression in Xenopus Oocytes—The zfCx52.6 construct subcloned into pCS2+ was used as the template for *in vitro* reactions to produce RNA for microinjection in *Xenopus* oocytes. The translation competence of the transcript was examined using a rabbit reticulocyte system supplemented with [^{35}S]methionine and labeled proteins were separated by SDS-gel electrophoresis. The connexin RNA directed the synthesis of a major polypeptide band, whose electrophoretic mobility was well in agreement with the molecular weight deduced from the amino acid sequence (data not shown). To determine the functional characteristics of zfCx52.6, defolliculated oocytes were injected with RNA and manually paired after removal of the vitelline envelope. All oocytes received antisense oligonucleotides against XenCx38 to minimize the contribution of the endogenous connexin to the recorded conductance (57, 58). ZfCx52.6 consistently induced the assembly of intercellular channels that resulted in levels of junctional currents that were two orders of magnitude greater than those measured in antisense-treated control pairs (Fig. 5).

Voltage Gating Behavior of zfCx52.6—To characterize the physiological behavior of channels composed of zfCx52.6, we first analyzed their voltage dependence. A representative family of junctional currents (I_j) evoked by voltage steps of opposite polarities and increasing amplitude (Fig. 6*A*) showed that I_j decreased with time for transjunctional voltages ≥ ±40 mV. Quantification of the voltage gating properties plotting the normalized conductance (G_j) *versus* transjunctional voltage (V_j) (Fig. 6*B*) demonstrated that the rate of decline over the duration of the voltage step tended to be greater with increasing driving force. Fitting the data of the normalized steady-state conductance from six pairs to a Boltzmann equation of the form given under "Materials and Methods" revealed a very slightly asymmetrical behavior (Table I). To analyze the kinetics of voltage gating, the current decay at V_js of +80 mV was fit to a second order exponential function (58). The rate of channel closure yielded time constants of 0.2 and 4.6 s for the fast (τ_1) and slow (τ_2) components, respectively, of the current decay. For comparison, junctional currents of the other retinal connexins skate Cx35 and perch Cx35 were also best fit by second-order exponential decay functions with time constants of 0.29, 0.32 (τ_1) and 2.53, 2.23 (τ_2) seconds respectively (13).

ZfCx52.6 Forms Voltage-activated Hemichannels—Since certain connexins have been shown to form functional hemichannels in particular in isolated teleost horizontal cells (58–65), we tested the ability of zfCx52.6 to induce non-junctional membrane conductance in single oocytes. Whole cell currents were recorded in response to depolarizing voltage steps that were sequentially imposed from a holding potential of −40 mV for a duration of 10 s. Oocytes expressing zfCx52.6 generated large outward currents that activated with the slow kinetics characteristic of hemichannels induced by other connexins (Fig. 7*A*, *top traces*). As expected, antisense-injected controls did not display any sign of voltage-activated outward currents (Fig. 7*A*, *middle traces*). Plots of the current/voltage relationships demonstrated that there was already a statistically significant ($p < 0.02$) 3-fold increase in the voltage-activated currents of zfCx52.6 hemichannels over control cells at a membrane potential of 0 mV (Fig. 7*B*). When the extracellular Ca^{2+} concentration was raised to 2.9 mM, hemichannel currents were drastically inhibited in a reversible fashion (Fig. 8, *A–C*). The analysis of a larger series of cells revealed that the effect of Ca^{2+} was statistically significant starting at a membrane potential of 20 mV ($p < 0.02$ by the paired Student's *t* test; $n = 5$). These data extend previous observations that the amplitude of hemichannel currents is critically dependent on extracellular Ca^{2+} concentration.

DISCUSSION

Molecular Diversity of Teleost Connexins—Our effort to characterize the composition of electrical synapses in the zebrafish

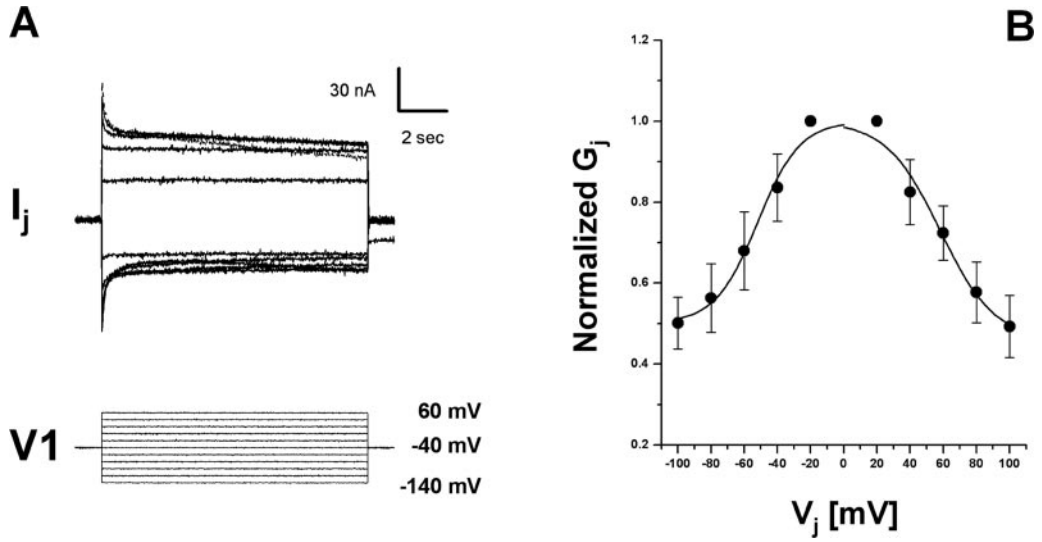

FIG. 6. **Voltage-gating behavior of gap junction channels formed by zfCx52.6.** *A*, time course of junctional currents recorded from oocyte pairs in response to transjunctional voltage (V_j) steps of opposite polarity applied in 20 mV increments from a holding potential of −40 mV. The currents reflect voltage-induced closure for V_j steps ≥ ±40 mV. *B*, plots describe the relationship of V_j to steady-state junctional conductance (G_j), normalized to the values obtained at ±20 mV. V_j induced an almost symmetrical channel closure for steps > ±20 mV. Results are shown as the mean ± S.E. of six oocyte pairs. The curves represent the best fits to Boltzmann equations, whose parameters are given in Table I.

TABLE 1
Boltzmann parameters of gap junction channels composed of zfC × 52.6

Junctional conductance (G_j) developed between pairs of Xenopus oocytes expressing different constructs was measured by dual voltage clamp in response to increasing transjunctional potentials (V_j) of opposite polarity and normalized to the maximum conductance (G_{jmax}, set as unity), as described under "Materials and Methods." Data were fit to a Boltzmann equation of the form given in the text. G_{jmin} is the minimum conductance value as estimated from the Boltzmann fit, and V_0 is the voltage at which half-maximal decrease of G_j is measured. The cooperativity constant (*A*), reflecting the voltage sensitivity of the channel, can also be expressed as the equivalent number (*n*) of electron charges moving through the transjunctional field. The plus and minus signs for V_j refer to the polarity of the voltage steps. These parameters were derived from 6 pairs whose mean conductance at the beginning of the experiment was 2.0 ± 0.7 μS at V_j ± 10 mV.

Channel	V_j	*A*	*n*	V_0
C × 52.6/C × 52.6	+	0.06	1.5	58
C × 52.6/C × 52.6	−	0.08	1.9	52

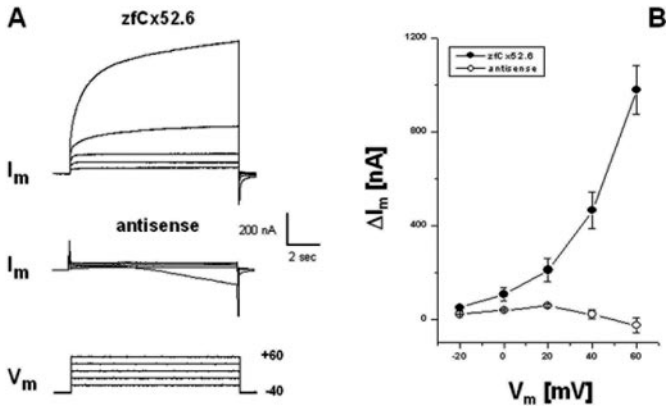

FIG. 7. **ZfCx52.6 forms voltage-activated hemichannels.** Oocytes pretreated with an oligonucleotide antisense to a sequence within the coding region of XenCx38 were injected with water, or zfCx52.6 RNA and whole cell membrane currents (I_m) were studied with a two-electrode voltage clamp in individual *Xenopus* oocytes. *A*, cells were depolarized in 20 mV steps of 10 s duration from a holding potential of −40 mV (*bottom traces*). Voltage-induced current recordings from oocytes expressing zfCx52.6 (*top traces*) exhibited large outward currents, whereas antisense-injected cells (*middle traces*) showed negligible membrane currents. *B*, plots of the current-voltage relationship of zfCx52.6 (*filled circles*) and antisense (*open circles*) injected oocytes. Whole cell membrane currents (ΔI_m) were measured 10 s after the imposition of a voltage step. At membrane potentials (V_m) ≥ 0 mV, expression of zfCx52.6-induced voltage-activated currents, which were significantly ($p < 0.02$ by the unpaired Student's *t* test) larger than those recorded from antisense-injected cells. Data shown are the mean ± S.E. of 10–11 oocytes.

retina has let led to the discovery of a wide variety of connexin genes that differ substantially at the molecular and functional level (18). The novel connexin zfCx52.6 is no exception from this rule. Its structure follows the general architectural rules of the connexin gene family with transmembrane regions highly homologous to those of other connexins and unique cytoplasmic portions. It is a member of the α-class of connexins, which is consistent with the finding of no introns within the coding region at the genomic level. Within the zfCx52.6 protein we identified conserved proline and cysteine residues in the connexin-appropriate positions (for comparison to other zebrafish connexins see Ref. 18). Furthermore, the striking abundance of the amino acid serine in the C-terminal domain along with numerous putative phosphorylation sites is an unusual feature shared only with zfCx55.5 (18). The expression of zfCx52.6 in a neuroblastoma cell line and *in vitro* transcription/translation experiments confirmed the predicted molecular weight (data not shown).

In the adult fish, zfCx52.6 expression was most prominent in the retina, where the expression level was at least 32-fold higher than in any of the other tissues examined. The sensitive quantitative real time RT-PCR demonstrated mRNA expression only at very low levels outside the retina, whereas conventional comparative RT-PCR did not detect this low expression levels. At the level of mRNA expression zfCx52.6 and the previously described zfCx55.5 share the identical organ distribution.

During development, zfCx52.6 expression is substantially up-regulated between 48 h and 72 h. In this period, major steps of neurogenesis/retinogenesis occur (66). In particular, we found a corresponding up-regulation of zfCx52.6 with the marker gene atonal5, which is a specific indicator for neuronal differentiation in the retina (40, 67).

The cellular localization of zfCx52.6 in the retina using two different techniques confirmed a specific localization of the mRNA at the border of the INL and OPL exactly at the site where horizontal cells are localized. In contrast to zfCx55.5,

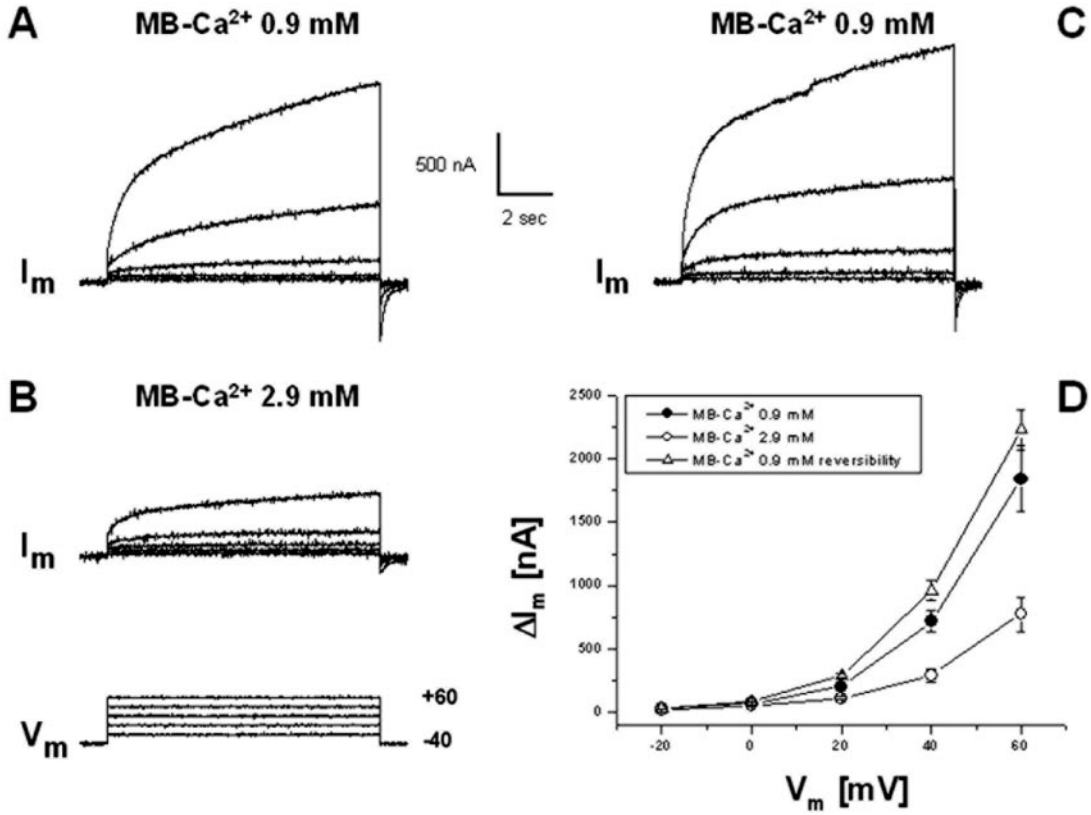

FIG. 8. **ZfCx52.6 hemichannels are gated by extracellular Ca^{2+} concentrations.** Cells were processed as described under "Materials and Methods," and whole cell membrane currents (I_m) were studied with a two-electrode voltage clamp in individual *Xenopus* oocytes. *A–C*, voltage-induced current recordings from oocytes expressing zfCx52.6 exhibited large outward currents (*A*), which were drastically reduced by raising the extracellular Ca^{2+} concentration to 2.9 mM (*B*). This effect was completely reversible by switching the medium back to standard MB (*C*). *D*, plots of the current-voltage relationship were obtained by measuring whole cell membrane currents (ΔI_m) 10 s after the imposition of a voltage step. The amplitude of the zfCx52.6 currents were significantly reduced ($p < 0.02$ by the paired Student's *t* test) starting at membrane potentials (V_m) ≥ 20 mV. Results are shown as the mean ± S.E. of three oocytes.

which has been described to show expression in cell clusters at the same localization (18) zfCx52.6 is expressed in linearly arranged cell lines covering most of the retinal circumference. This topological distribution strongly indicates that the expression of zfCx52.6 is restricted to horizontal cells.

The evolutionary relationship of zfCx52.6 to other connexin genes is low when compared with other zebrafish connexins or against all phyla. Most interestingly, our analysis points to the fact that zfCx52.6 has no obvious ortholog in higher vertebrates. Again, this is a feature shared with zfCx55.5, where no obvious functional equivalent in higher vertebrates has been identified so far. This observation raises the question why evolution does conserve some connexins, *e.g.* zfCx43 (18) or skate Cx35 (9), but not others like zfCx52.6 or zfCx55.5 (18). One potential explanation is that functional convergence has occurred during the evolution of the connexin gene family. Alternatively, electrical transmission in neuronal tissues of teleosts might have evolved to a higher degree requiring a more diversified molecular composition. However, the most likely cause for the increased number of connexin genes in zebrafish is the large scale genome duplication that has occurred in the teleost lineage between 200 and 400 million years ago (68, 69).

The site-restricted expression of zfCx55.5 and zfCx52.6 in the retina suggests that this neuronal tissue is endowed with a broader spectrum of functionally specialized connexins than mammalian retinas, where only Cx36 has been unambiguously identified to be neuronally expressed. Given the fact that both zfCx52.6 and zfCx55.5 show peculiar electrophysiological and molecular properties the issue of functional evolution of electrically coupled neuronal networks in fish retina becomes an appealing explanation. Unraveling the functional meaning of this molecular diversification awaits further studies utilizing model systems like the Mauthner cell paradigm (70).

Functional Properties of zfCx52.6—Functional expression studies in transfected Neuro2A cells revealed that the unitary conductance of zfCx52.6 channels was about 40pS. Previous studies have shown that in the fish retina, horizontal cell gap junction channels exhibit unitary conductances in the 40–60 pS range (71) consistent with the apparent horizontal cell localization of the zfCx52.6 transcript as shown in Fig. 3.

Functional expression studies in single or paired *Xenopus* oocytes illustrated further details of the biophysical behavior of this novel connexin. ZfCx52.6 was capable of forming intercellular channels in homotypic configuration. The voltage gating properties of zfCx52.6 revealed greater voltage sensitivity than Cx35/Cx36, which was clearly illustrated by comparing the values of transjunctional voltage (V_0) required to elicit a conductance midway between G_{jmax} and G_j (*e.g.* around 55mV for zfCx52.6 and 100mV for mCx36). It was also noted that the junctional current decay was slightly asymmetrical, *i.e.* the rate of decline over the duration of the voltage step tended to be greater for negative values of V_j. Thus, fitting the data from six pairs to a Boltzmann equation showed that the V_0 values of 58 mV for positive V_js, and a value of 52 mV for negative V_js. A minor asymmetric voltage sensitivity has been previously reported also for other fish connexins (18, 72). Finally, the kinetics of voltage induced closure measured for zfCx52.6 showed that the decay of junctional currents was best fit by a second order exponential function, with a fast component that matched the values of Cx35/Cx36, whereas the slow transitions

from high to low conductance were much slower (cf. with Ref. 13). This voltage dependence is similar to those reported for junctional currents in fish horizontal cells (71).

Interestingly, we found that zfCx52.6 forms hemichannels when expressed in single oocytes. Outward currents were already significantly activated at 0 mV, increased dramatically at positive membrane potentials and were inhibited in reversible fashion by increasing extracellular Ca^{2+} concentrations. This basic feature seems to be shared by other fish connexins expressed in the retina, including skate and perchCx35 (13, 62) as well as zfCx55.5,[3] thereby suggesting that it may serve a specific function in retinal neurons. In this context, it is interesting to note, that it has been recently proposed that connexin hemichannels underlie horizontal cell feedback to cones in the teleost retina (73). It remains to be established whether hemichannels expressed in other cell types of the inner nuclear layer may also affect synaptic transmission between different classes of neurons.

Finally, the large number of phosphorylation sites present in the C-terminal tail makes zfCx52.6 an attractive candidate to test the modulation of channel activity by second messenger pathways that activate distinct protein kinases. The functional properties of zfCx52.6 should allow us to compare the gating mechanisms of hemichannels to those of the complete intercellular channels and to identify to what extent post-translational modifications affect channel gating, and which are the molecular determinants involved.

Acknowledgments—We thank Marie-Madeleine Gabellec for skillful technical assistance, Monika Birkelbach for help with the photographic work, and Helga Schulze for help with the zebrafish colony.

REFERENCES

1. Bruzzone, R., White, T. W., and Paul, D. L. (1996) *Eur. J. Biochem.* **238,** 1–27
2. Harris, A. L. (2001) *Q. Rev. Biophys.* **34,** 325–472
3. Willecke, K., Eiberger, J., Degen, J., Eckardt, D., Romualdi, A., Guldenagel, M., Deutsch, U., and Sohl, G. (2002) *Biol. Chem.* **383,** 725–737
4. Bennett, M. V. L., Barrio, T. A., Bargiello, T. A., Spray, D. C., Hertzberg, E., and Sáez, J. C. (1991) *Neuron* **6,** 305–320
5. Dermietzel, R., and Spray, D. C. (1993) *Trend Neurosci.* **16,** 186–192
6. Zoidl, G., and Dermietzel, R. (2002) *Cell Tissue Res.* **310,** 137–142
7. Galarreta, W., and Hestrin, S. (1999) *Nature* **402,** 72–75
8. Gibson, J. R., Beierlein, M., and Connors, B. W. (1999) *Nature* **402,** 75–79
9. O'Brien, J., Al-Ubaidi, M. R., and Ripps, H. (1996) *Mol. Biol. Cell* **7,** 233–243
10. O'Brien, J., Bruzzone, R., White, T. W., Al-Ubaidi, M. R., and Ripps, H. (1998) *J. Neurosci.* **18,** 7625–7637
11. Condorelli, D. F., Parenti, R., Spinella, F., Salinaro, A. T., Belluardo, N., Cardile, V., and Cicirata, F. (1998) *Eur. J. Neurosci.* **10,** 1202–1208
12. Sohl, G., Degen, J., Teubner, B., and Willecke, K. (1998) *FEBS Lett.* **428,** 27–31
13. Al-Ubaidi, M. R., White, T. W., Ripps, H., Poras, I., Avner, P., Gomes, D., and Bruzzone, R. (2000) *J. Neurosci. Res.* **59,** 813–826
14. Feigenspan, A., Teubner, B., Willecke, K., and Weiler, R. (2001) *J. Neurosci.* **21,** 230–239
15. Hormuzdi, S. G., Pais, I., LeBeau, F. E. N., Towers, S. K., Rozov, A., Buhl, E. H., Whittington, M. A., and Monyer, H. (2001) *Neuron* **31,** 487–495
16. Deans, M. R., Volgyi, B., Goodenough, D. A., Bloomfield, S. A., and Paul, D. L. (2002) *Neuron* **36,** 703–712
17. Meier, C., Petrasch-Parwez, E., Habbes, H. W., Teubner, B., Guldenagel, M., Degen, J., Sohl, G., Willecke, K., and Dermietzel, R. (2002) *Histochem. Cell Biol.* **117,** 461–471
18. Dermietzel, R., Kremer, M., Paputsoglu, G., Stang, A., Skerrett, I. M., Gomes, D., Srinivas, M., Janssen-Bienhold, U., Weiler, R., Nicholson, B. J., Bruzzone, R., and Spray, D. C. (2000) *J. Neurosci.* **20,** 8331–8343
19. Sohl G., Guldenagel M., Traub O., and Willecke K. (2000) *Brain Res. Rev.* **32,** 138–145
20. White, T. W., and Bruzzone, R. (2000) *Brain Res. Rev.* **32,** 130–137
21. Vaney, D. I. (1994) *Prog. Ret. Eye Res.* **13,** 301–353
22. Vaney, D. I. (1996) in *Gap Junctions in the Nervous System* (Spray, D. C., and Dermietzel, R., eds) pp. 79–102, R. G. Landes, Austin, TX
23. Weiler, R. (1996) in *Gap Junctions in the Nervous System* (Spray, D. C., and Dermietzel, R., eds) pp. 103–121, R. G. Landes, Austin, TX
24. Becker, D., Bonness, V., and Mobbs, P. (1998) *Cell Biol. Int.* **22,** 781–792
25. Vaney, D. I. (1991) *Neurosci. Lett.* **125,** 187–190
26. Vaney, D. I. (1993) *Proc. R. Soc. Lond. B. Biol. Sci.* **252,** 93–101
27. Vaney, D. I., Nelson, J. C., and Pow, D. V. (1998) *J. Neurosci.* **18,** 10594–10602
28. Guldenagel, M., Ammermuller, J., Feigenspan, A., Teubner, B., Degen, J., Sohl, G., Willecke, K., and Weiler, R. (2001) *J. Neurosci.* **21,** 6036–6044
29. Veruki, M. L., and Hartveit, E. (2002) *J. Neurosci.* **22,** 10558–10566
30. Veruki, M. L., and Hartveit, E. (2002) *Neuron* **33,** 935–946
31. Piccolino, M., Neyton, J., and Witkovsky, P. (1982) *Proc. Natl. Acad. Sci. U. S. A.* **79,** 3671–3675
32. Lasater, E. M. (1987) *Proc. Natl. Acad. Sci. U. S. A.* **84,** 7319–7323
33. DeVries, S. H., and Schwartz, E. A. (1989) *J. Physiol.* (*Lond*) **414,** 351–375
34. Miyachi, E., and Murakami, M. (1989) *J. Physiol.* (*Lond.*) **419,** 213–224
35. Hampson, E. C. Vaney, D. I., and Weiler, R. (1992) *J. Neurosci.* **12,** 4911–4922
36. Qian, H., and Ripps, H. (1992) *J. Gen. Physiol.* **100,** 457–478
37. Lu, C., Zhang, D-Q., and McMahon, D. G. (1999) *Vis. Neurosci.* **16,** 811–818
38. Hampson, E. C., Weiler, R., and Vaney, D. I. (1994) *Proc. R. Soc. Lond. B. Biol. Sci.* **255,** 67–72
39. Mills, S. L., and Massey, S. C. (1995) *Nature* **377,** 734–738
40. Vetter, M. L., and Brown, N. L. (2001) *Semin. Cell Dev. Biol.* **12,** 491–498
41. Janssen-Bienhold, U., Nagel, H., and Weiler, R. (1993) *Eur. J. Neurosci.* **5,** 584–593
42. Haefliger, J-A., Bruzzone, R., Jenkins, N. A., Gilbert, D. J., Copeland, N. G., and Paul D. L. (1992) *J. Biol. Chem.* **267,** 2057–2064
43. Zoidl, G., Meier, C., Petrasch-Parwez, E., Zoidl, C., Habbes, H-W., Kremer, M., Srinivas, M, Spray, D. J, and Dermietzel, R. (2002) *J. Neurosci. Res.* **69,** 448–465
44. Russwurm, M., Mergia, E., Zoidl, G., and Koesling, D. (2003) *Cell. Signaling* **15,** 189–195
45. Gillen, C., Gleichmann, M., Greiner-Petter, R., Zoidl, G., Kupfer, S., Bosse, F., Auer, J., and Müller, H. W. (1996) *Eur. J. Neurosci.* **8,** 405–414
46. Olmsted, J. B., Carlson, K., Klebe, R., Ruddle, F., and Rosenbaum, J. R. J. (1970) *Proc. Natl. Acad. Sci. U. S. A.* **65,** 129–136
47. Hopperstad, M. G., Srinivas, M., and Spray, D. C. (2000) *Biophys. J.* **79,** 1954–1966
48. Swenson, K. I., Jordan, J. R., Beyer, E. C., and Paul, D. L. (1989) *Cell* **57,** 145–155
49. Mitropoulou, G., and Bruzzone, R. (2003) *J. Neurosci. Res.* **15,** 147–157
50. Methfessel, C., Witzemann, V., Takahashi, T., Mishina, M., Numa, S., and Sakmann, B. (1986) *Pflügers Arch.* **407,** 577–588
51. Spray, D. C., Harris, A. L., and Bennett, M. V. L. (1981) *J. Gen. Physiol.* **77,** 75–94
52. Wilders, R., and Jongsma, H. J. (1992) *Biophys. J.* **63,** 942–953
53. Milks, L. C., Kumar, N. M., Houghton, R., Unwin, N., and Gilula, N. B. (1988) *EMBO J.* **7,** 2967–2975
54. Yeager, M., Unger, V. M., and Falk, M. M. (1998) *Curr. Opin. Struct. Biol.* **8,** 517–524
55. Altschul, S. F., Gish, W., Miller, W., Myers, E. W., and Lipman, D. J. (1990) *J. Mol. Biol.* **215,** 403–410
56. Kimmel, C. B., Ballard, W. W., Kimmel, S. R., Ullmann, B., and Schilling, T. F. (1995) *Dev. Dyn.* **203,** 253–310
57. Scheer, N., Groth, A., Hans, S., and Campos-Ortega, J. A. (2001) *Development* **128,** 1099–1107
58. Barrio, L. C. Suchyna, T., Bargiello, T., Xu, L., Roginski, R. S., Bennett, M. V., and Nicholson, B. J. (1991) *Proc. Natl. Acad. Sci. U. S. A.* **88,** 8410–8414
59. Bruzzone, R., Haefliger, J. A., Gimlich, R. L., and Paul, D. L. (1993) *Mol. Biol. Cell.* **4,** 7–20
60. Hennemann, H., Suchyna, T., Lichtenberg-Frate, H., Jungbluth, S., Dahl, E., Schwarz, J., Nicholson, B. J., and Willecke, K. (1992) *J. Cell Biol.* **117,** 1299–1310
61. Li, H., Liu, T., Lazrak, A., Peracchia, C., Goldberg, G. S., Lampe, P. D., and Johnson, R. G. (1996) *J. Cell Biol.* **134,** 1019–1030
62. Castro, C., Gomez-Hernandez, J. M., Silander, K., and Barrio, L. C. (1999) *J. Neurosci.* **19,** 3752–3760
63. White, T. W., Deans, M. R., O'Brien, J., Al-Ubaidi, M. R., Goodenough, D. A., Ripps, H., and Bruzzone, R. (1999) *Eur. J. Neurosci.* **11,** 1883–1890
64. Quist, A. P., Rhee, S. K., Lin, H., and Lal, R. (2000) *J. Cell Biol.* **148,** 1063–1074
65. DeVries, S. H., and Schwartz, E. A. (1992) *J. Physiol.* (*Lond.*) **445,** 201–230
66. Mueller, T., and Wullimann, M. F. (2003) *Brain Res. Dev. Brain Res.* **140,** 137–155
67. Masai, I., Stemple, D. L., Okamoto, H., and Wilson, S. W. (2000) *Neuron* **27,** 251–263
68. Taylor, J. S., Braasch, I., Frickey, T., Meyer, A., and Van de Peer, Y. (2003) *Genome Res.* **13,** 382–390
69. Van de Peer, Y., Taylor, J. S., and Meyer, A. (2003) *J. Struct. Funct. Genomics* **3,** 65–73
70. Pereda, A. E., Bell, T. D., and Faber, D. S. (1995) *J. Neurosci.* **15,** 5943–5955
71. McMahon, D. G. (1994) *J. Neurosci.* **14,** 1722–1734
72. Wagner, T. L., Beyer, E. C., and McMahon, D. G. (1998) *Vis. Neurosci.* **15,** 1173
73. Kaamermans, M., Fahrenfort, I., Schultz, K., Janssen-Bienhold, U., Sjoerdsma, T., and Weiler, R. (2001) *Science* **292,** 1178–1180

[3] G. Mitropoulou and R. Bruzzone, unpublished observations.

Molecular Cloning and Functional Expression of zfCx52.6: A NOVEL CONNEXIN WITH HEMICHANNEL-FORMING PROPERTIES EXPRESSED IN HORIZONTAL CELLS OF THE ZEBRAFISH RETINA

Georg Zoidl, Roberto Bruzzone, Svenja Weickert, Marian Kremer, Christiane Zoidl, Georgia Mitropoulou, Miduturu Srinivas, David C. Spray and Rolf Dermietzel

J. Biol. Chem. 2004, 279:2913-2921.
doi: 10.1074/jbc.M304850200 originally published online October 28, 2003
